

COGNITIVE NEUROSCIENCE

A broadly tuned network for affective body language in the macaque brain

Jessica Taubert^{1,2+*}, Shruti Japee^{1+*}, Amanda Patterson¹, Hannah Wild¹, Shivani Goyal¹, David Yu¹, Leslie G. Ungerleider^{1‡}

Body language is a powerful tool that we use to communicate how we feel, but it is unclear whether other primates also communicate in this way. Here, we use functional magnetic resonance imaging to show that the body-selective patches in macaques are activated by affective body language. Unexpectedly, we found these regions to be tolerant of naturalistic variation in posture as well as species; the bodies of macaques, humans, and domestic cats all evoked a stronger response when they conveyed fear than when they conveyed no affect. Multivariate analyses confirmed that the neural representation of fear-related body expressions was species-invariant. Collectively, these findings demonstrate that, like humans, macaques have body-selective brain regions in the ventral visual pathway for processing affective body language. These data also indicate that representations of body stimuli in these regions are built on the basis of emergent properties, such as socio-affective meaning, and not just putative image properties.

INTRODUCTION

Like all primates, humans use facial expressions to communicate with each other. Unlike any other primates, however, we walk on two legs. Obligate bipedalism ensures that our upper limbs are almost always available to help us communicate, and recent studies have shown that our body postures and hand gestures are as informative about our internal state as our facial expressions (1, 2). Functional magnetic resonance imaging (fMRI) has revealed two discrete body-selective areas in the occipitotemporal cortex—the extrastriate body area (3) and the fusiform body area (4). Both areas are activated more by affective body expressions than neutral body expressions (5, 6). Expressions related to fear are thought to elicit a particularly strong response from body-selective areas because perceiving and recognizing fear in others is essential for quickly reacting to potential threats in the environment (7, 8). Although these observations all hint at the function and evolutionary origins of the body-selective areas, at present, there is no evidence that other primates share our sensitivity to affective body language.

Like humans, macaques have two functionally defined body-selective regions positioned along the ventral visual pathway, referred to as the “body patches” (9, 10). These body patches are positioned on the lower bank of the superior temporal sulcus (sts; Fig. 1A), and they form a tightly interconnected network that runs parallel to the face patch network (11). Although body patches have been shown to be driven by a diverse range of visual stimuli, including images of headless macaque bodies, macaque body parts, headless human bodies, and bodies of other mammals and birds (12–14), we do not yet understand whether these patches serve the same function as the body-selective areas in the human brain. An interesting

question, therefore, is whether the macaque body patches play a role in processing affective body language.

RESULTS

Experiment 1

To characterize the response of the body patches to body expressions, we first localized the body patches in four macaques using fMRI (Fig. 1A). The contrast between bodies and the nonbody categories delineated two patches: the middle body patch (MBP) and the anterior body patch (ABP) in all four subjects (for details, see the Supplementary Materials; Fig. 1A). Next, we measured the response of these patches to body expressions using a standard set of stimuli (15) that have been previously used to drive activity in the human body-selective areas (6, 16). We found that both the MBP and the ABP were more activated by fearful body expressions than neutral body expressions (both P values < 0.001 ; Fig. 1B), and they were also more activated by angry body expressions than neutral body expressions (both P values < 0.001 ; Fig. 1B). As expected, the fear condition elicited the highest median response from both patches (Fig. 1, B and C). The positive happy expressions yielded mixed results across patches and subjects (fig. S2); the voxels in MBP responded more to happy body expressions than neutral body expressions ($P = 0.006$; Fig. 1B), but the voxels in ABP responded equally to happy and neutral body expressions ($P = 0.49$; Fig. 1B). These observations establish a strong functional homology between the human and macaque brain by showing that the same exact body stimuli engage the body-selective network in both species such that the strongest and most consistent neural responses were elicited by fearful body expressions.

Experiment 2

Although the results of the first experiment demonstrate that affective body expressions elicit a stronger response from the body patch network than neutral body expressions, it is important to confirm that this result generalizes to more naturalistic stimuli (17). Since signals from conspecifics ought to be more relevant and meaningful

Copyright © 2022
The Authors, some
rights reserved;
exclusive licensee
American Association
for the Advancement
of Science. No claim to
original U.S. Government
Works. Distributed
under a Creative
Commons Attribution
NonCommercial
License 4.0 (CC BY-NC).

¹Section on Neurocircuitry, Laboratory of Brain and Cognition, National Institute of Mental Health, Bethesda, MD 20892, USA. ²School of Psychology, The University of Queensland, Brisbane, QLD 4072, Australia.

[†]These authors contributed equally to this work.

[‡]Deceased.

*Corresponding author. Email: j.taubert@uq.edu.au (J.T.); shruti.japee@nih.gov (S.J.)

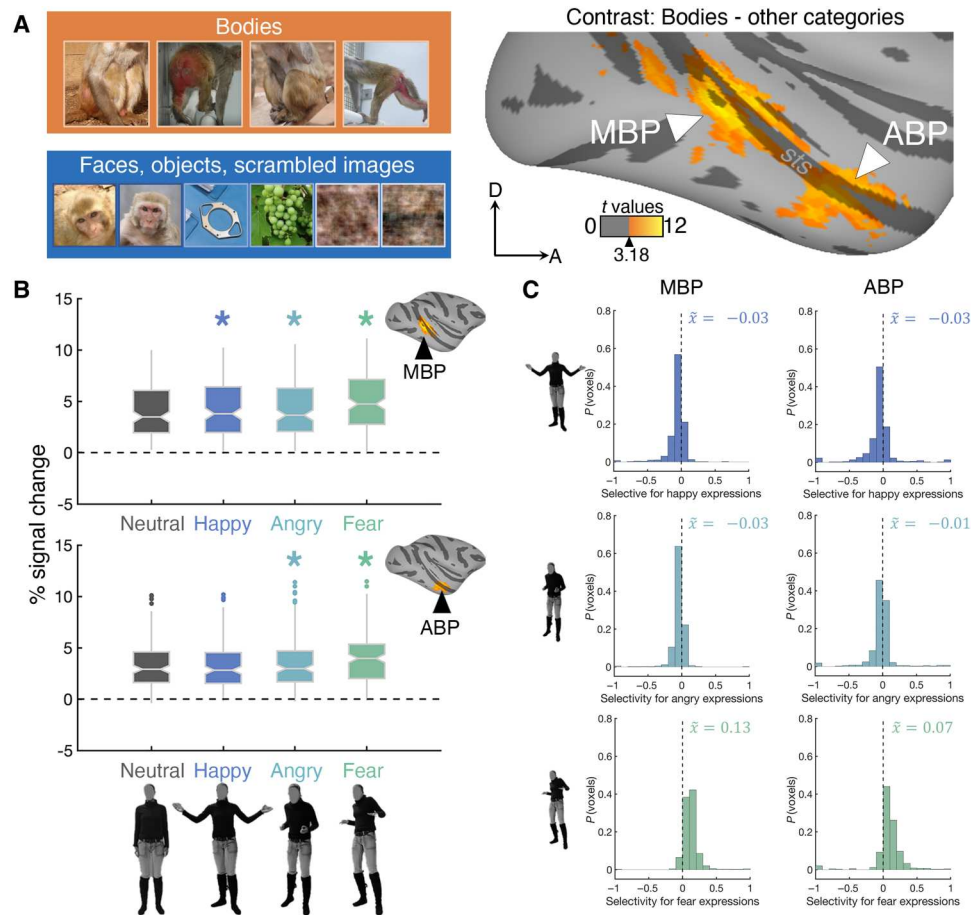


Fig. 1. Affective body language recruits the body patch network in the macaque brain. (A) Left, illustrative examples of the stimuli used to localize the body patches in all four subjects. Right, lateral view of an inflated macaque cortex (right hemisphere) with the group data ($N = 4$) from the independent localizer experiment. The contrast between bodies and the other three stimulus categories yielded the relative location of the body patches along the superior temporal sulcus (sts). The statistical threshold was set at $P = 0.05$ (uncorrected). (B) Top: The percent signal change from baseline for middle body patch (MBP) voxels as a function of expression condition. Asterisks indicate the experimental conditions with a median response greater than the neutral condition. The median response across the four conditions is as follows: \bar{x} neutral = 3.47%, \bar{x} happy = 3.78%, \bar{x} angry = 3.64%, and \bar{x} fear = 4.73%. Bottom: A box plot visualizing the percent signal change from baseline for anterior body patch (ABP) voxels as a function of expression condition. Asterisks indicate conditions with a median response greater than the corresponding neutral condition. The median % signal change across the four conditions is as follows: \bar{x} neutral = 2.9%, \bar{x} happy = 2.81%, \bar{x} angry = 2.97%, and \bar{x} fear = 3.96%. For individual subject data and results, see fig. S2. (C) Distributions of “expression selectivity” among MBP voxels and ABP voxels (top, happy selectivity defined as $[\bar{x} \text{ happy} - (\bar{x} \text{ other expressions})] / |\bar{x} \text{ happy}| + |(\bar{x} \text{ other expressions})|$]; middle, angry selectivity defined as $[\bar{x} \text{ angry} - (\bar{x} \text{ other expressions})] / |\bar{x} \text{ angry}| + |(\bar{x} \text{ other expressions})|$]; bottom, fear selectivity defined as $[\bar{x} \text{ fear} - (\bar{x} \text{ other expressions})] / |\bar{x} \text{ fear}| + |(\bar{x} \text{ other expressions})|$]. Scores above zero indicate that a voxel responded more strongly to a specific expression (happy, angry, or fear) than to the other three expressions.

than signals from allospecifics, we tested whether photographs of macaques differed in their affective body language. We created a stimulus set composed of naturalistic, wild-type macaque bodies, validated by behavioral ratings collected from human participants (Fig. 2A). Then, we measured fMRI activity in four macaques while they viewed macaque bodies that varied in both expression (neutral versus fearful) and orientation (upright versus inverted). For each subject, we selected the 40 voxels with the highest body-selective index from the cortical regions of interest—ABP and MBP, and the amygdala (Fig. 2C; see the Supplementary Materials).

For MBP, we found main effects of expression ($F_{1,159} = 632.04$, $P < 0.001$, $\eta_p^2 = 0.8$) and orientation ($F_{1,159} = 138.56$, $P < 0.001$, $\eta_p^2 = 0.47$). The interaction was also significant ($F_{1,159} = 7.05$, $P = 0.009$,

$\eta_p^2 = 0.04$), justifying the two simple contrasts to test for discrete effects (i.e., fearful > neutral) within each level of orientation. The critical P values for these tests were corrected using the Bonferroni rule (Fig. 2C). The same pattern of results was also seen for both ABP (expression, $F_{1,159} = 585.32$, $P < 0.001$, $\eta_p^2 = 0.79$; orientation, $F_{1,159} = 69.34$, $P < 0.001$, $\eta_p^2 = 0.30$; and interaction, $F_{1,159} = 9.71$, $P = 0.002$, $\eta_p^2 = 0.06$) and the amygdala (expression, $F_{1,159} = 203.85$, $P < 0.001$, $\eta_p^2 = 0.56$; orientation, $F_{1,159} = 3.91$, $P = 0.05$, $\eta_p^2 = 0.02$; and interaction, $F_{1,159} = 9.84$, $P = 0.002$, $\eta_p^2 = 0.06$). Thus, using naturalistic stimuli, we found that viewing the bodies of conspecifics displaying fear-related behaviors activates the body patches and the amygdala more so than viewing the bodies of resting conspecifics. The reliability of these body expression effects was confirmed using

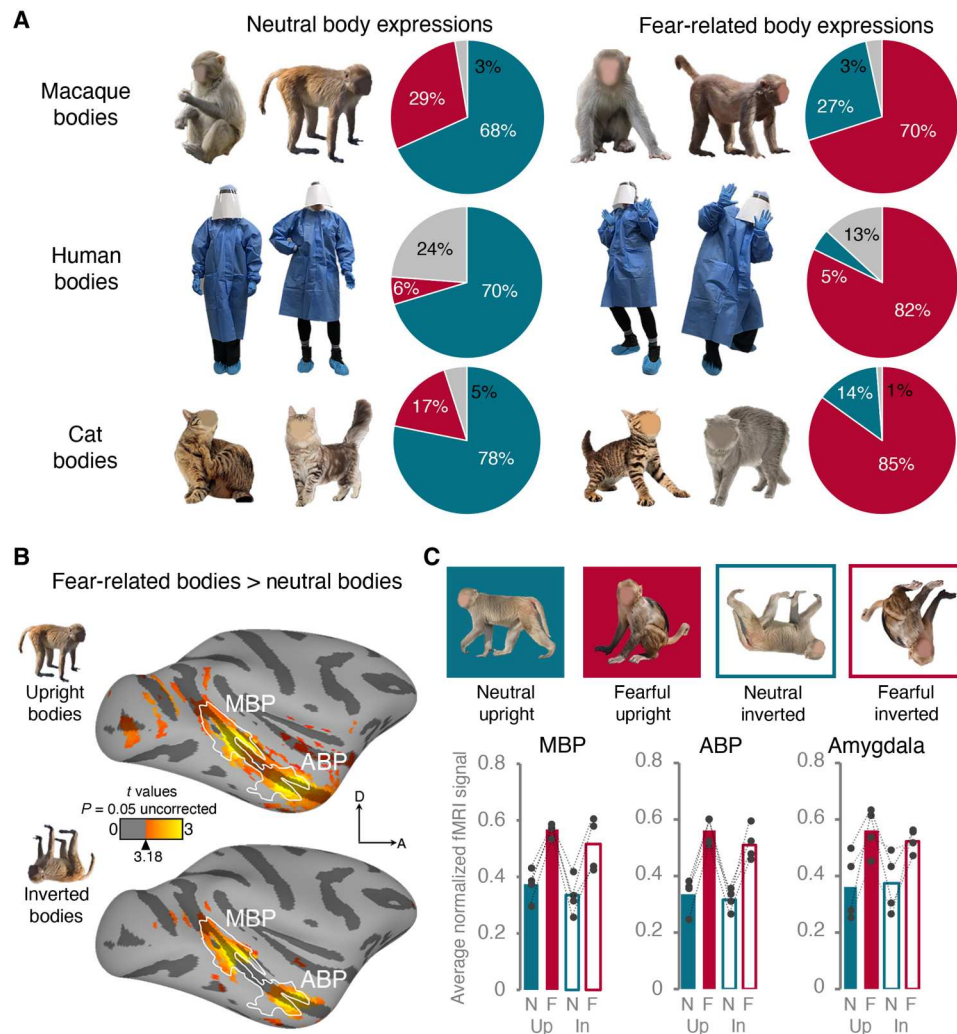


Fig. 2. Fear-related body language in naturalistic, wild-type photographs of conspecifics drives activity in the body patches. (A) Behavioral validation of the body postures assigned to the neutral (left) and fearful (right) conditions. Next to two illustrative examples of each stimulus species is the distribution of categorical responses (blue shows the proportion of responses that indicated stimuli were neutral, red shows the proportion of responses that indicated stimuli were fearful, and gray shows the proportion of responses that indicated another category). For complete stimulus set and details of behavioral validation experiment, see fig. S1. (B) Top: Lateral view of an inflated macaque cortex (right hemisphere) with the contrast between fearful upright and neutral upright conspecific bodies projected onto the surface ($N = 4$). The statistical threshold was set at $P = 0.05$ (uncorrected). The white outline indicated the relative location of the body-selective patches at the group level. Bottom: Lateral view of the left hemisphere with the contrast between fearful-inverted and neutral-inverted conspecific bodies projected on the surface. (C) Bar graphs displaying the average normalized fMRI signal elicited from body-selective voxels across the three regions of interest (left, MBP; middle, ABP; and right, the amygdala) after pooling the data across subjects. Error bars reflect \pm SEM. Lines with circles indicate individual subject results. Colors reflect experimental condition. Follow-up contrasts uncovered similar biases toward fearful stimuli [MBP upright stimuli, mean difference between fearful and neutral bodies (M_{diff}) = 0.2, SE = 0.008, $P < 0.001$; MBP inverted stimuli, M_{diff} = 0.18, SE = 0.008, $P < 0.001$; ABP upright stimuli, M_{diff} = 0.22, SE = 0.009, $P < 0.001$; ABP inverted stimuli, M_{diff} = 0.19, SE = 0.01, $P < 0.001$; amygdala upright stimuli, M_{diff} = 0.19, SE = 0.01, $P < 0.001$; and amygdala inverted stimuli, M_{diff} = 0.15, SE = 0.02, $P < 0.001$].

leave-one-run-out searchlight analyses (fig. S3). Furthermore, in a separate experiment ($N = 2$), we confirmed that the effects of expression reported in experiment 2 were driven by perceived expression (fearful versus neutral), not perceived speed (fast versus slow; see Materials and Methods and fig. S4).

The results thus far all show that both macaque and human body expressions drive activity in the body patch network, although these two species have different phenotypic body parts and stereotypical body postures. These observations suggest that the body patch network is broadly tuned to the perception of affect, with a high

tolerance for variation in physical appearance. Does this tolerance extend to the affective body language of another, less familiar species? To test this, we compared expression effects across three levels of stimulus species—conspecifics (macaques), familiar allospecifics (humans in laboratory coats), and unfamiliar allospecifics (domestic cats; Fig. 2A). We scanned three subjects over multiple sessions; in each scan session, we presented them with either human or cat bodies and we compared the results to those from the previous macaque body experiment (i.e., experiment 2).

Experiment 3

Figure 3A shows the average effects of expression for upright bodies on a cortical surface. For the two body patches, MBP and ABP, we computed “expression effects” for upright and inverted bodies, separately, by subtracting the response to neutral body expressions from that to fear-related body expressions. We assessed the impact of species (macaques, humans, and cats) and orientation (upright bodies and inverted bodies) on the expression effect in each region of interest using a 3×2 repeated measures analysis of variance (Fig. 3B). For both body patches, we found a main effect of species (MBP, $F_{2,238} = 263.74$, $P < 0.001$, $\eta_p^2 = 0.69$; ABP, $F_{2,238} = 314.63$, $P < 0.001$, $\eta_p^2 = 0.73$) and orientation (MBP, $F_{1,119} = 45.84$, $P < 0.001$, $\eta_p^2 = 0.28$; ABP, $F_{1,119} = 52.52$, $P < 0.001$, $\eta_p^2 = 0.31$), with greater responses to upright bodies than inverted bodies. We also found a significant interaction between species and orientation (MBP, $F_{2,238} = 31.05$, $P < 0.001$, $\eta_p^2 = 0.21$; ABP, $F_{2,238} = 6.45$, $P = 0.002$, $\eta_p^2 = 0.05$). As expected, for the MBP, we found that macaque bodies elicited a larger effect of expression than human or cat bodies, regardless of whether the body stimuli were presented upright [macaques versus humans, mean difference (M_{diff}) = 1.29, SE = 0.09, $P < 0.001$; macaques

versus cats, $M_{\text{diff}} = 1.83$, SE = 0.1, $P < 0.001$] or inverted (macaques versus humans, $M_{\text{diff}} = 1.5$, SE = 0.1, $P < 0.001$; macaques versus cats, $M_{\text{diff}} = 1.32$, SE = 0.1, $P < 0.001$; Fig. 3B). This was also true for the ABP (upright macaques versus humans, $M_{\text{diff}} = 1.07$, SE = 0.08, $P < 0.001$; upright macaques versus cats, $M_{\text{diff}} = 1.49$, SE = 0.08, $P < 0.001$; inverted macaques versus humans, $M_{\text{diff}} = 1.08$, SE = 0.09, $P < 0.001$; inverted macaques versus cats, $M_{\text{diff}} = 1.21$, SE = 0.08, $P < 0.001$; Fig. 3B). When the stimuli were presented upright, human bodies elicited a larger expression effect than unfamiliar cat bodies (MBP, $M_{\text{diff}} = 0.53$, SE = 0.04, $P < 0.001$; ABP, $M_{\text{diff}} = 0.43$, SE = 0.05, $P < 0.001$; Fig. 3B). Yet, when the stimuli were presented upside down, we found no evidence that human and cat bodies evoked differential expression effects (MBP, $M_{\text{diff}} = -0.17$, SE = 0.07, $P = 0.02$; ABP, $M_{\text{diff}} = 0.14$, SE = 0.06, $P = 0.02$; Fig. 3B). These observations likely reflect the fact that human bodies have a canonical upright stance that can be disrupted by picture-plane inversion.

Next, we examined the correlation between expression effects in the ventral visual pathway and found that voxels differentially activated by fear-related body expressions were species-invariant (Fig. 4A). We used cross-decoding as a critical test of species

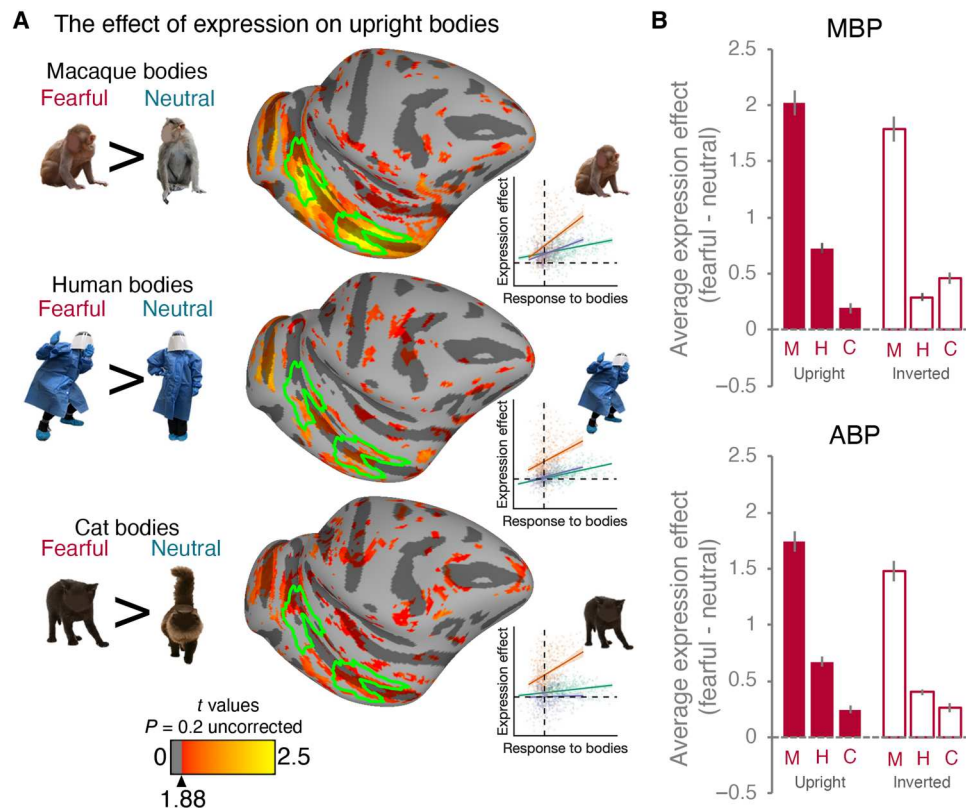


Fig. 3. Response to fear-related body language is not species-specific. (A) Contrast between fearful upright bodies and neutral upright bodies (group-level analysis; $N = 3$) for all three stimulus species (top, macaque bodies; middle, human bodies; bottom, cat bodies). Cortical surfaces are rotated to visualize the lower bank of the sts, and a green outline indicates the relative location of the body patches. Corresponding scatterplots show the correlation between the differential response to bodies (bodies – non-bodies) in the localizer experiment and the expression effect for upright stimuli in experiment 2, for all voxels in the ventral visual pathway (separate colors represent three separate subjects). In all cases, we found that the more responsive to bodies a voxel was, the greater the effect of expression (macaque bodies, P values < 0.001 ; human bodies, P values < 0.001 ; cat bodies, P values < 0.001), except for one subject while viewing cat bodies ($P = 0.59$). (B) Bar graphs showing the average expression effects elicited from body-selective voxels in the two regions of interest (top, MBP; bottom, ABP). Error bars reflect \pm SEM. All expression effects were above zero for upright (one-sample t tests, t values range from 19.2 to 4.4, all P values < 0.001 , two-tailed) and inverted stimuli (t values range from 16.7 to 5.8, all P values < 0.001 , two-tailed).

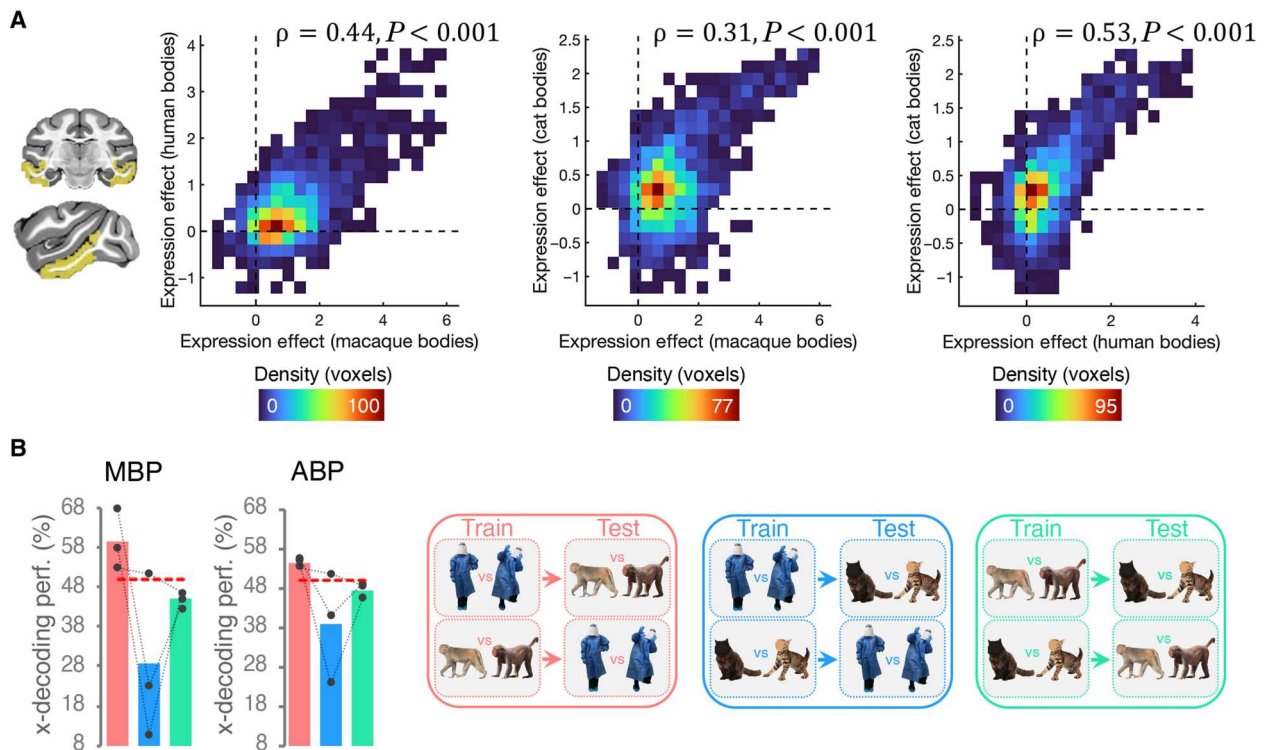


Fig. 4. Perceived affect dominates the neural representation of body stimuli. (A) Two-dimensional density plots showing the correlations between expression effects (left, human versus macaque bodies; middle, cat versus macaque bodies; right, cat versus human bodies) for all voxels in the ventral visual pathway (the mask used is illustrated on the far left). Spearman's rho tests were used to measure the strength of the relationship between expression effects. (B) Bar graph shows cross-decoding performance, averaged across subjects (the individual subject results are plotted as black dotted lines). The red dashed line indicates chance-level performance (50%). Only data from the upright conditions were used in this analysis. The results show that decoding performance was above chance ($\geq 50\%$) for all three subjects only when the classifier was provided macaque body and human body data (pink bars).

invariance. To do this, a linear classifier was trained on the fMRI brain activation patterns evoked by one species (e.g., macaque neutral bodies versus macaque fearful bodies) and tested on the activation patterns for a different species (e.g., human neutral bodies versus human fearful bodies). This analysis requires that the classifier must generalize not only across unique datasets but also across different stimuli (e.g., humans versus macaque bodies) to correctly classify expression (neutral or fearful). This eliminates the possibility that decoding performance reflects low-level image properties or even the phenotypic features of a particular species, such as the blue laboratory coat worn by actors in the human stimuli.

We found above-chance cross-decoding performance in all three subjects, and both body patches, for macaque bodies versus human bodies (MBP, average decoding performance = 59.77%; ABP, average decoding performance = 54.41%; Fig. 4B). This result solidifies the conclusion that the body patches are broadly tuned to highly variable body expressions. By contrast, the cross-decoding analysis failed for macaque bodies versus cat bodies (MBP, average decoding performance = 28.5%; ABP, average decoding performance = 38.81%; Fig. 4B) and human bodies versus cat bodies (MBP average decoding performance = 44.99%; ABP average decoding performance = 47.53%; Fig. 4B)—results consistent with the smaller effect size associated with cat expressions seen in the univariate analysis (Fig. 3B). Cats might have elicited smaller expression effects because the subjects were less familiar with their physical form, suggesting that perceptual expertise plays an

important role in the visual processing of socio-affective cues. That said, the significant expression effect for cat bodies (Fig. 3), together with the correlations in Fig. 4A, indicates that, even without long-term training or perceptual expertise, highly unfamiliar body expressions activate the same regions of the ventral visual pathway as highly familiar body expressions. This degree of generalization speaks to function and developmental origins of body selectivity in primates; an advantageous consequence of having a broadly tuned body-selective network is that it promotes a universal sensitivity to fear-related signals.

DISCUSSION

A popular theory in cognitive neuroscience posits that humans, as social primates, are sensitive to body expressions (particularly fear-related body expressions) because they help us prepare our own bodies for potential action (5, 7, 18–20). Until now, however, evidence of any continuity across the primate order was lacking. Here, we provide strong evidence that viewing fear-related body expressions increases activity in the macaque brain. Thus, rhesus macaques share our sensitivity to body expressions (17). This key neural correlate creates a direct, functional parallel between the body-selective network in the macaque brain and the body-selective areas in the human brain and is consistent with the view that other nonhuman primates are also equipped to recognize affective body language.

We found that expression effects were evident in both the MBP and the ABP, indicating that there is no division of labor within the body patch network. This is somewhat unexpected when you consider the division of labor within the adjacent face patch network; expressions and other dynamic facial attributes are thought to drive activity in a subset of face patches (21–23). Thus, our observations here suggest that body stimuli are processed in a unique computational pipeline where the processing of expressions is ubiquitous. Although consistent with a large literature (9–12, 14, 24), the reasons why body expressions would be processed separately from facial expressions remain unknown and warrant further investigation (25).

Although, in these experiments, we labeled the expression conditions as “fearful” and “neutral” (because this is how they were rated by human participants), it is possible that the neural correlates we observed represent responses to other socio-affective attributes such as valence or arousal (26–29). Admittedly, in the first experiment, we found evidence that all expressions (i.e., happy, angry, and fearful) differentially activated the body patches (Fig. 1 and fig. S2). Thus, it is clear that the body patches are not singularly tuned to fear or fear-related behaviors. Rather, these data indicate that activity in the body patches is driven by body postures that signal a change in affective state from neutral. More research is needed to determine the extent to which fear-related behaviors are unique compared to other behaviors associated with high arousal and negative valence. Nonetheless, these results demonstrate that the macaque body patches play a role in processing affective body language.

Last, our data show that this broadly tuned network for affective body language is robust to variation in physical form and image properties. The standard view of neural representations of visual stimuli in the ventral visual pathway is that they are dominated by physical similarity (i.e., visual inputs that appear similar will be encoded similarly) (30–33). However, these data challenge this view by demonstrating that the naturalistic expressions conveyed by different animal species elicit the same response from the same voxels, despite animals having differently shaped bodies subject to different biomechanical limits. Therefore, neural representations in the macaque body patches, at the temporal resolution afforded by fMRI, are dominated by the perception of affect (i.e., visual inputs conveying similar emotions are encoded similarly). We note that evidence of abstract affective coding has also been observed in a previous cross-modal study (34). It follows that activity in the ventral visual pathway might be better characterized by more complex, higher-level attributes, such as socio-affective meaning, rather than low-level visual properties.

MATERIALS AND METHODS

All procedures were in accordance with the *Guide for the Care and Use of Laboratory Animals* and the National Institutes of Health Animal Research Advisory Committee Guidelines. All procedures were approved by the National Institute of Mental Health Animal Care and Use Committee.

Subjects

Four adult rhesus macaques (*Macaca mulatta*, 6 to 13 years of age and weighing between 5.6 and 10.3 kg at the time of testing) participated in these experiments (subjects H and J were males; S and R were females). We kept the sample size to the smallest number possible that would still allow for scientific inference. Previous reports

of similar fMRI experiments on this species have demonstrated that a sample size of 3 to 4 is sufficient (15, 17, 21, 23, 35–38). The subjects were originally acquired from a breeding facility in the United States where they were housed in large social groups until their transfer to the National Institute of Mental Health at the age of ~4 years. After that, they were housed in a colony room with auditory and visual contact with at least 20 other conspecifics. All subjects also had daily interactions with human caregivers, NIH staff, and research trainees. Food was available ad libitum, and water was controlled as needed to maintain testing motivation, with their weight remaining above 85% of baseline.

Each subject was surgically implanted with a headpost under sterile conditions using isoflurane anesthesia. After recovery, the subjects were slowly acclimated to the experimental procedure; first, they were trained to sit calmly in a plastic restraint chair and fixate a small (0.5° to 0.7° visual angle) red central dot for long durations (~8 min). Fixation within a circular window (radius 2° of visual angle) centered over the fixation dot resulted in juice delivery. The length of fixation that was required for juice delivery during training and scan sessions varied randomly throughout the length of a run. The average time between rewards was typically 2 s (± 300 ms) but varied depending on the animal's behavior.

Data acquisition

Before each scanning session, an exogenous contrast agent (monocrystalline iron oxide nanocolloid or MION) was injected into the femoral vein to increase the signal-to-noise ratio (35, 36, 39–41). MION doses were determined independently for each subject (~8 to 10 mg/kg).

Structural and functional data were acquired in a 4.7-T, 60-cm vertical scanner (Bruker Biospec, Ettlingen, Germany) equipped with a Bruker S380 gradient coil. Subjects viewed the visual stimuli projected onto a screen above their head through a mirror positioned in front of their eyes. We collected whole-brain images with a four-channel transmit-and-receive radiofrequency coil system (Rapid MR International, Columbus, OH). A low-resolution anatomical scan was also acquired in the same session to serve as an anatomical reference [modified driven equilibrium Fourier transform (MDEFT) sequence: voxel size, 1.5 mm by 0.5 mm by 0.5 mm; field of view (FOV), 96 mm by 48 mm; matrix size, 192 \times 96; echo time (TE), 3.95 ms; and repetition time (TR), 11.25 ms]. Functional echo planar imaging (EPI) scans were collected as 42 sagittal slices with an in-plane resolution of 1.5 mm by 1.5 mm and a slice thickness of 1.5 mm. The TR was 2.2 s, and the TE was 16 ms (FOV, 96 mm by 54 mm; matrix size, 64 \times 36 m; and flip angle, 75°). Eye position was recorded using a magnetoresistance-compatible infrared camera (MRC Systems, Heidelberg, Germany) fed into MATLAB (MathWorks, version R2018b) via a DATApixx hub (VPixx Technologies, Vision Science Solutions). In separate sessions, we also acquired high-resolution T1-weighted whole-brain anatomical scans under sedation in a 4.7-T Bruker scanner with an MDEFT sequence. Imaging parameters were as follows: voxel size, 0.5 mm by 0.5 mm by 0.5 mm; TE, 4.9 ms; TR, 13.6 ms; and flip angle, 14°. These scans were used to create a high-resolution template for each subject.

fMRI preprocessing

All EPI data were analyzed using AFNI software (<http://afni.nih.gov/afni>) (42). Preprocessing procedures have been outlined in

detail in previous studies (21, 36, 37). Raw images were first converted from Bruker into AFNI data file format. The data collected in a single session were corrected for static magnetic field inhomogeneities using the PLACE algorithm (43). The time series data were then slice time-corrected and realigned to the volume with the minimum outliers. All the data for a given subject were aligned to the corresponding high-resolution template for that subject, allowing for the combination of data across multiple sessions. The first two volumes of data in each EPI sequence were discarded. The volume-registered data were then spatially smoothed with a 3-mm Gaussian kernel and rescaled to reflect percentage signal change from baseline. To combine data across subjects, structural and functional scans for each subject were spatially normalized to the National Institute of Mental Health (NIMH) Macaque Template (NMT version 2.0) (44) using a nonlinear warping procedure.

Localization of the body patches

To localize the body patches, bilaterally, in each of the four subjects, we used an independent functional localizer experiment. This experiment had a standard on/off block design with four conditions: macaque bodies, macaque faces, objects, and phase-scrambled bodies (for illustrative examples, see Fig. 1A). During a “stimulus on” block, 20 images were presented one at a time for 900 ms and were followed by a 200-ms interstimulus interval. Every run began with 4.4 s of fixation, or 2 volumes, and thus, in each run, we collected 82 volumes of data. Each stimulus was presented to awake fixating subjects in full Red-Green-Blue (RGB) color and on a square canvas (10° of visual angle in height). We removed any run from the analysis where the monkey did not fixate within a 4° window for more than 50% of the time.

Once the data were moved into the NMT space, the body patches were identified in each of the four subjects using the following contrast: bodies – (scenes + objects + phase-scrambled bodies). A statistical threshold of $q = 0.0001$ [false discovery rate (FDR)] revealed both body patches (the MBP and the ABP; Fig. 1A) in all eight hemispheres. To define the amygdala region of interest, we first applied a mask of the amygdala obtained from the Subcortical Atlas of Rhesus Macaque (45) to the whole-brain data and then used the following contrast: bodies – phase-scrambled bodies (with a voxel-wise statistical threshold of $q = 0.0001$, FDR).

This process yielded regions of interest that varied greatly in size (i.e., 20–213 voxels). Therefore, we used two different strategies to ensure that each subject contributed equally to the experimental outcomes. For univariate analyses, we selected 20 voxels from each region of interest (per hemisphere). This was accomplished by first calculating a body selectivity index [BSI = $(\beta_{\text{bodies}} - \beta_{\text{non-bodies}}) / (|\beta_{\text{bodies}}| + |\beta_{\text{non-bodies}}|)$] for every voxel within the larger regions of interest and then selecting the 20 voxels with the highest BSI value. This means that our univariate analyses were limited to the most body-selective neuronal populations within the regions of interest that were defined with a singular statistical threshold. We then normalized the data for each region of interest before performing fixed-effects analyses using the min-max normalization method.

However, multivariate analyses are designed to probe patterns of activation across contiguous voxels. Thus, for the decoding analyses performed on the data from three subjects, we kept the data in individual template space and used the same contrast [i.e., bodies – (scenes + objects + phase-scrambled bodies)] to identify the peak

activations in the inferior temporal cortex. Then, we defined the distinct regions of interest by drawing spheres with a 4-mm radius centered on the two peak activations corresponding to the MBP and ABP in all six hemispheres.

Experiment 1

Stimuli

A set of 72 grayscale images of human bodies were selected from the BEAST stimulus set (Bodily Expressive Action Stimulus Set) (15). Images for nine male actors and nine female actors were chosen, whose validation accuracy exceeded 78%. Thus, this set was composed of 18 neutral bodies, 18 happy bodies, 18 angry bodies, and 18 fearful bodies (Fig. 1B and fig. S1). For each of the body images, we created a second copy by flipping the image horizontally. This was to prevent any systematic asymmetry in body postures from favoring one hemifield. Thus, there were 36 stimuli per condition. Stimuli were resized to the same height and placed on a square canvas ($10^\circ \times 10^\circ$ of visual angle).

Experimental design and procedure

Experiment 1 used a high-powered on/off block design. Every run began with two dummy pulses and then 4.4 s of fixation before the onset of the experimental blocks. A central red fixation spot (0.4° diameter) remained on the screen for the entire duration of a run. The subjects were tasked with fixating on the red spot (within a fixation window that was 4° of visual angle in diameter). As long as the subjects maintained their fixation within the window, they received a juice reward approximately once every 2 s (± 400 ms).

The 36 stimuli in each condition were presented one at a time in a block at the center of a gray screen behind the fixation spot. The order of the stimuli and the order of conditions in any given run were determined at random. Stimulus presentation was 900 ms with an interstimulus interval of 200 ms. Thus, all stimulation blocks were 39.6 s in duration, and each was followed by a 39.6-s fixation period. Each run lasted 321.2 s, during which we collected 146 volumes of data.

Subjects had to fixate within the fixation window for at least 70% of the run time for the data to be included in the analysis. Subject H completed 12 runs above this behavioral criterion in a single session, subject J completed 7 runs also in a single session, subject S completed 15 runs in a single session, and subject R completed 9 runs above the behavioral criterion also in a single session.

Experiments 2 and 3

Macaque stimuli

For experiment 2, which used macaque bodies as stimuli, we selected photographs of macaques interacting naturally with other macaques in large groups (photographs taken and curated by J.T. or sourced from the public domain; creative commons license, CC BY). Thirty-six photographs of macaques were selected on the basis of the presence or absence of a silent bared teeth display (18 neutral, 18 fearful; Fig. 1B and fig. S1). We removed the background from these photographs, replacing it with a mid-gray color. Facial features were removed with the blur function in Adobe Photoshop (v2020). Each stimulus was then resized to fit on a square canvas ($10^\circ \times 10^\circ$ of visual angle) depending on its longest dimension. For each of the macaque bodies, we created a second copy by flipping the image horizontally. Therefore, in total, there were 36 stimuli per condition (see fig. S1). The inverted conditions—*inverted neutral bodies* and *inverted fearful bodies*—were created by

rotating each stimulus 180° in the picture plane. The stimuli were validated by collecting categorization and expressiveness ratings from 19 raters. Participants were shown the 72 images in random order and asked to categorize them as either fearful, neutral, other, or do not know. They were also asked to provide a rating for how strong the perceived affect was using the following choices: neutral, very weak, weak, moderate, strong, and very strong. Overall, participants correctly classified fearful and neutral body expressions with 70 and 68% accuracy, respectively. In addition, fearful stimuli were on the average rated as moderate or higher intensity over 59% of the time.

We note that the behavioral validation of these stimuli was meant to mirror the validation of stimulus sets used in previous human research (15). However, these kinds of forced choice paradigms are flawed. For instance, one concern is that we used Western-centric categorical labels to describe “emotional states” that likely do not translate across cultures or species. It follows that this task forced the participants to assign category labels that perhaps did not properly characterize the intended signal of the macaques being photographed. These are important concerns highlighting the need to better understand how affective body language is produced and used by different primates.

Human stimuli

For experiment 3, our goal was to use images of human bodies dressed in a way that would be more familiar to the subjects. Therefore, we took two photographs of nine models per condition (one neutral and one fearful). The models wore full personal protective gear, including a laboratory coat, surgical cap/hair net, gloves, and booties. The face shield was modified so that no facial features were visible. We removed the background from these photographs, replacing it with a mid-gray color. The stimuli were resized to the same height and placed on a square canvas (10° × 10° of visual angle). Thus, we had 18 unique neutral bodies and 18 unique fearful bodies (Fig. 1B and fig. S1). For each of the bodies, we again created a second copy by flipping the image horizontally; in total, there were 36 stimuli per condition. As with the macaque stimuli, the human stimuli for the two inverted conditions were created by rotating each stimulus 180° in the picture plane. The stimuli were validated by collecting categorization and expressiveness ratings from 50 workers on Amazon Mechanical Turk. Participants were shown the 18 images in random order and asked to categorize them as either angry, fearful, happy, neutral, other, or do not know. They were also asked to provide a rating for how strong the perceived affect was using the following choices: no emotion, very weak, weak, moderate, strong, and very strong. Overall, participants correctly classified fearful and neutral body expressions with 82 and 70% accuracy, respectively. In addition, fearful stimuli were on the average rated as moderate intensity or higher over 67% of the time.

Cat stimuli

We collected 36 images of cats from the public domain (creative commons license CC BY). Eighteen cat images displayed no affect, while the other 18 were fearful of something in the environment (see Fig. 1B and fig. S1). We carefully removed the background information, replacing it with a mid-gray color. Then, facial features were removed with the blur function in Adobe Photoshop (v2020) before each stimulus was resized to fit on a square canvas (10° × 10° of visual angle) depending on its longest dimension. For each of the cat body images, we created a second copy by flipping the image horizontally. Therefore, in total, there were 36

stimuli per condition (see fig. S1). The inverted conditions were created by rotating each stimulus 180° in the picture plane. The stimuli were validated by collecting categorization and expressiveness ratings from 14 raters. Participants were shown the 72 images in random order and asked to categorize them as either fearful, neutral, other, or do not know. They were also asked to provide a rating for how strong the perceived affect was using the following choices: neutral, very weak, weak, moderate, strong, and very strong. Overall, participants correctly classified fearful and neutral body expressions with 85 and 78% accuracy, respectively. In addition, fearful stimuli were on the average rated as moderate or higher intensity over 60% of the time.

General design and procedure

For stimuli of all three species, we presented four conditions in an on/off block-design. In all three cases, the conditions were upright neutral bodies, upright fearful bodies, inverted neutral bodies, and inverted fearful bodies. For each run, the order of the conditions and the order of stimuli were determined at random. The timing parameters used were identical to those described above for experiment 1.

Subjects had to fixate within the fixation window for at least 70% of the total run time for the data to be included in the analysis. For macaque bodies, subject H successfully completed 8 runs in two scan sessions, subject J completed 9 runs in a single session, subject S completed 13 runs in two sessions, and subject R completed 8 runs above the behavioral criterion in two scan sessions. For human bodies, subject H completed 24 runs in two sessions, subject S completed 21 runs in a single session, and subject R completed 17 runs in two scan sessions. Last, for cat bodies, subject H completed 19 runs in a single session, subject S completed 22 runs in a single session, and subject R completed 14 runs in two scan sessions. We note that the collection of more data was impossible because of COVID precautions that were in place to protect the staff, trainees, and subjects.

Motion control experiment

Stimuli

The 16 of the fearful macaque bodies and 16 of the neutral macaque bodies from experiment 2 were selected for the motion control experiment based on ratings of perceived motion (on a five-point scale, whereby 0 was “not moving at all” and 4 was “moving a lot”) collected from 10 human participants. The eight fearful bodies with the highest average score were selected for the “fast and fearful” condition, and the eight fearful bodies with the lowest average score were selected for the “slow and fearful” condition. Similarly, the eight neutral bodies with the highest average score were selected for the “fast and neutral” condition, and the eight neutral bodies with the lowest average score were selected for the “slow and neutral” condition. Next, we presented these four conditions in a standard block design fMRI experiment to two subjects, using the same stimulus-timing parameters as in previous experiments. Both subjects (subjects S and R) had to fixate for at least 70% of the total run time for the run to be included in the analysis. Both subjects were scanned on one occasion, and both completed 22 runs in total. For results, see fig. S4.

Supplementary Materials

This PDF file includes:

Figs. S1 to S4

REFERENCES AND NOTES

- H. Aviezer, Y. Trope, A. Todorov, Body cues, not facial expressions, discriminate between intense positive and negative emotions. *Science* **338**, 1225–1229 (2012).
- M. Poyo Solanas, M. Zhan, M. Vaessen, R. Hortensius, T. Engelen, B. de Gelder, Looking at the face and seeing the whole body. Neural basis of combined face and body expressions. *Soc. Cogn. Affect. Neurosci.* **13**, 135–144 (2018).
- P. E. Downing, Y. Jiang, M. Shuman, N. Kanwisher, A cortical area selective for visual processing of the human body. *Science* **293**, 2470–2473 (2001).
- R. F. Schwarzlose, C. I. Baker, N. Kanwisher, Separate face and body selectivity on the fusiform gyrus. *J. Neurosci.* **25**, 11055–11059 (2005).
- M. V. Peelen, P. E. Downing, The neural basis of visual body perception. *Nat. Rev. Neurosci.* **8**, 636–648 (2007).
- N. Hadjikhani, B. de Gelder, Seeing fearful body expressions activates the fusiform cortex and amygdala. *Curr. Biol.* **13**, 2201–2205 (2003).
- B. de Gelder, J. Snyder, D. Greve, G. Gerard, N. Hadjikhani, Fear fosters flight: A mechanism for fear contagion when perceiving emotion expressed by a whole body. *Proc. Natl. Acad. Sci. U.S.A.* **101**, 16701–16706 (2004).
- C. C. R. J. van Heijnsbergen, H. K. Meeren, J. Grèzes, B. de Gelder, Rapid detection of fear in body expressions, an ERP study. *Brain Res.* **1186**, 233–241 (2007).
- I. D. Popivanov, J. Jastorff, W. Vanduffel, R. Vogels, Stimulus representations in body-selective regions of the macaque cortex assessed with event-related fMRI. *Neuroimage* **63**, 723–741 (2012).
- M. A. Pinsk, K. DeSimone, T. Moore, C. G. Gross, S. Kastner, Representations of faces and body parts in macaque temporal cortex: A functional MRI study. *Proc. Natl. Acad. Sci. U.S.A.* **102**, 6996–7001 (2005).
- E. Premereur, J. Taubert, P. Janssen, R. Vogels, W. Vanduffel, Effective connectivity reveals largely independent parallel networks of face and body patches. *Curr. Biol.* **26**, 3269–3279 (2016).
- I. D. Popivanov, J. Jastorff, W. Vanduffel, R. Vogels, Heterogeneous single-unit selectivity in an fMRI-defined body-selective patch. *J. Neurosci.* **34**, 95–111 (2014).
- I. D. Popivanov, J. Jastorff, W. Vanduffel, R. Vogels, Tolerance of macaque middle STS body patch neurons to shape-preserving stimulus transformations. *J. Cogn. Neurosci.* **27**, 1001–1016 (2015).
- M. A. Pinsk, M. Arcaro, K. S. Weiner, J. F. Kalkus, S. J. Inati, C. G. Gross, S. Kastner, Neural representations of faces and body parts in macaque and human cortex: A comparative fMRI study. *J. Neurophysiol.* **101**, 2581–2600 (2009).
- B. de Gelder, J. Van den Stock, The bodily expressive action stimulus test (BEAST). Construction and validation of a stimulus basis for measuring perception of whole body expression of emotions. *Front. Psychol.* **2**, 181 (2011).
- J. Ren, R. Ding, S. Li, M. Zhang, D. Wei, C. Feng, P. Xu, W. Luo, Features and extra-striate body area representations of diagnostic body parts in anger and fear perception. *Brain Sci.* **12**, 466 (2022).
- B. de Gelder, S. Partan, The neural basis of perceiving emotional bodily expressions in monkeys. *Neuroreport* **20**, 642–646 (2009).
- B. de Gelder, Towards the neurobiology of emotional body language. *Nat. Rev. Neurosci.* **7**, 242–249 (2006).
- B. de Gelder, A. W. de Borst, R. Watson, The perception of emotion in body expressions. *Wiley Interdiscip. Rev. Cogn. Sci.* **6**, 149–158 (2015).
- M. V. Peelen, A. P. Atkinson, F. Andersson, P. Vuilleumier, Emotional modulation of body-selective visual areas. *Soc. Cogn. Affect. Neurosci.* **2**, 274–283 (2007).
- J. Taubert, S. Japee, A. P. Murphy, C. T. Tardiff, E. A. Koele, S. Kumar, D. A. Leopold, L. G. Ungerleider, Parallel processing of facial expression and head orientation in the macaque brain. *J. Neurosci.* **40**, 8119–8131 (2020).
- W. Freiwald, B. Duchaine, G. Yovel, Face processing systems: From neurons to real-world social perception. *Annu. Rev. Neurosci.* **39**, 325–346 (2016).
- H. Zhang, S. Japee, A. Stacy, M. Flessert, L. G. Ungerleider, Anterior superior temporal sulcus is specialized for non-rigid facial motion in both monkeys and humans. *Neuroimage* **218**, 116878 (2020).
- C. Fisher, W. A. Freiwald, Whole-agent selectivity within the macaque face-processing system. *Proc. Natl. Acad. Sci. U.S.A.* **112**, 14717–14722 (2015).
- J. Taubert, J. B. Ritchie, L. G. Ungerleider, C. I. Baker, One object, two networks? Assessing the relationship between the face and body-selective regions in the primate visual system. *Brain Struct. Funct.* **227**, 1423–1438 (2022).
- L. F. Barrett, R. Adolphs, S. Marsella, A. M. Martinez, S. D. Pollak, Emotional expressions reconsidered: Challenges to inferring emotion from human facial movements. *Psychol. Sci. Public Interest* **20**, 1–68 (2019).
- E. Bliss-Moreau, Constructing nonhuman animal emotion. *Curr. Opin. Psychol.* **17**, 184–188 (2017).
- J. A. Russell, Is there universal recognition of emotion from facial expression? A review of the cross-cultural studies. *Psychol. Bull.* **115**, 102–141 (1994).
- J. M. Carroll, J. A. Russell, Do facial expressions signal specific emotions? Judging emotion from the face in context. *J. Pers. Soc. Psychol.* **70**, 205–218 (1996).
- P. Bao, L. She, M. McGill, D. Y. Tsao, A map of object space in primate inferotemporal cortex. *Nature* **583**, 103–108 (2020).
- S. Bracci, J. B. Ritchie, I. Kalfas, H. P. Op de Beeck, The ventral visual pathway represents animal appearance over animacy, unlike human behavior and deep neural networks. *J. Neurosci.* **39**, 6513–6525 (2019).
- H. Op de Beeck, J. Wagemans, R. Vogels, Inferotemporal neurons represent low-dimensional configurations of parameterized shapes. *Nat. Neurosci.* **4**, 1244–1252 (2001).
- G. E. Rice, D. M. Watson, T. Hartley, T. J. Andrews, Low-level image properties of visual objects predict patterns of neural response across category-selective regions of the ventral visual pathway. *J. Neurosci.* **34**, 8837–8844 (2014).
- M. V. Peelen, A. P. Atkinson, P. Vuilleumier, Supramodal representations of perceived emotions in the human brain. *J. Neurosci.* **30**, 10127–10134 (2010).
- B. E. Russ, D. A. Leopold, Functional MRI mapping of dynamic visual features during natural viewing in the macaque. *Neuroimage* **109**, 84–94 (2015).
- J. Taubert, S. G. Wardle, C. T. Tardiff, E. A. Koele, S. Kumar, A. Messinger, L. G. Ungerleider, The cortical and subcortical correlates of face pareidolia in the macaque brain. *Soc. Cogn. Affect. Neurosci.* **17**, 965–976 (2022).
- J. Taubert, S. G. Wardle, C. T. Tardiff, A. Patterson, D. Yu, C. I. Baker, Clutter substantially reduces selectivity for peripheral faces in the macaque brain. *J. Neurosci.* **42**, 6739–6750 (2022).
- Q. Zhu, K. Nelissen, J. van den Stock, F.-L. de Winter, K. Pauwels, B. de Gelder, W. Vanduffel, M. Vandenbulcke, Dissimilar processing of emotional facial expressions in human and monkey temporal cortex. *Neuroimage* **66**, 402–411 (2013).
- W. Vanduffel, D. Fize, J. B. Mandeville, K. Nelissen, P. van Hecke, B. R. Rosen, R. B. H. Tootell, G. A. Orban, Visual motion processing investigated using contrast agent-enhanced fMRI in awake behaving monkeys. *Neuron* **32**, 565–577 (2001).
- J. Taubert, G. Van Belle, W. Vanduffel, B. Rossion, R. Vogels, Neural correlate of the Thatcher face illusion in a monkey face-selective patch. *J. Neurosci.* **35**, 9872–9878 (2015).
- S. H. Park, B. E. Russ, D. B. T. McMahon, K. W. Koyano, R. A. Berman, D. A. Leopold, Functional subpopulations of neurons in a macaque face patch revealed by single-unit fMRI mapping. *Neuron* **95**, 971–981.e5 (2017).
- R. W. Cox, AFNI: Software for analysis and visualization of functional magnetic resonance neuroimages. *Comput. Biomed. Res.* **29**, 162–173 (1996).
- Q.-S. Xiang, F. Q. Ye, Correction for geometric distortion and N/2 ghosting in EPI by phase labeling for additional coordinate encoding (PLACE). *Magn. Reson. Med.* **57**, 731–741 (2007).
- J. Seidlitz, C. Sponheim, D. Glen, F. Q. Ye, K. S. Saleem, D. A. Leopold, L. Ungerleider, A. Messinger, A population MRI brain template and analysis tools for the macaque. *Neuroimage* **170**, 121–131 (2018).
- R. Hartig, D. Glen, B. Jung, N. K. Logothetis, G. Paxinos, E. A. Garza-Villarreal, A. Messinger, H. C. Evrard, The Subcortical Atlas of the Rhesus Macaque (SARM) for neuroimaging. *Neuroimage* **235**, 117996 (2021).

Acknowledgments: We thank the Neurophysiology Imaging Facility Core (NIMH, National Institute of Neurological Disorders and Stroke, National Eye Institute) for functional and anatomical MRI scanning, with special thanks to A. P. Murphy, C. Zhu, and F. Ye for technical assistance. We also thank C. Baker (NIMH) for invaluable advice. **Funding:** This research was supported by the Intramural Research Program of the National Institute of Mental Health (NIMH; grants ZIAMH002918 to L.G.U.) and the Australian Research Council (FT200100843 to J.T.). **Author contributions:** J.T., S.J., and L.G.U. designed the study. A.P., H.W., and S.G. collected and curated the stimulus set. S.J., H.W., and S.G. collected the behavioral data. J.T., A.P., and D.Y. collected the MRI data. J.T. and S.J. analyzed the results and wrote the paper. All authors edited the manuscript. **Competing interests:** The authors declare that they have no competing interests. **Data and materials availability:** All data needed to evaluate the conclusions in the paper are present in the paper and/or the Supplementary Materials. Source data and materials generated in this study have been deposited in an Open Science Framework database found at <https://osf.io/v3mzr/>.

Submitted 27 June 2022

Accepted 27 October 2022

Published 25 November 2022

10.1126/sciadv.add6865